

**LOW-VELOCITY COLLISION DYNAMICS ON EARTH VS. SMALL-BODIES.** C. Sunday<sup>1,2</sup>, N. Murdoch<sup>1</sup>, M. Drilleau<sup>1</sup>, A. Wilhelm<sup>1</sup>, P. Michel<sup>2</sup>, <sup>1</sup>Institut Supérieur de l'Aéronautique et de l'Espace (ISAE-SUPAERO), Toulouse, France (cecily.sunday@isae-supaeo.fr), <sup>2</sup>Université Côte d'Azur, Observatoire de la Côte d'Azur, Centre National de la Recherche Scientifique (CNRS), Laboratoire Lagrange, Nice, France.

**Introduction:** Recent missions like Hayabusa2 and OSIRIS-REx have taught us surprising lessons on how to interact with regolith in micro-gravity [1, 2]. While these experiences will surely help with the operation planning for future small-body missions like Dart [3], Hera [4], and MMX [5], we are still unable to predict with certainty what will happen the next time we set a lander down on the surface of an asteroid.

In this study, we examine how low-velocity impacts into granular surfaces differ between terrestrial and low-gravity environments. We present the results from experimental and numerical impact tests that have been conducted under different gravity levels and compare the observed behaviors against an existing theoretical collision model. We also investigate the suitability of the Froude number for describing these collisions.

**Impact experiments and simulations:** Low-velocity impact experiments were performed by dropping a 10 cm diameter spherical projectile into a container filled with either 1.5 mm or 10 mm diameter glass beads, where the initial drop height of the projectile was varied in order to obtain different collision velocities. The tests were executed under terrestrial gravity using a static laboratory set-up and then again under reduced-gravity conditions using the drop-tower at ISAE-Supaéro [6]. More information on the impact experiments can be found in [7].

In order to expand upon the analysis presented in [7], we conducted a series of low-velocity impact simulations using the open-source code Chrono and the soft-sphere Discrete Element Method [8]. The simulation set-up replicates the terrestrial gravity experiment, where a 31.5 cm diameter bucket is filled with 10 mm diameter glass beads. We determined the coefficients of rolling and spinning friction for the simulated glass beads by tuning the numerical results to match experimental data. All of the other simulation parameters and material properties match those of glass beads as described in [8].

**Data analysis:** In this study, we investigate the influence of gravity on three parameters that are often used to describe collision behavior: the peak acceleration of the projectile ( $a_{\text{peak}}$ ), the maximum penetration depth of the projectile ( $z_{\text{stop}}$ ), and the total duration of the collision ( $t_{\text{stop}}$ ). The position, velocity, and acceleration profiles of the projectile are obtained using either accelerometer data from the experimental

trials or direct outputs from the numerical simulations. In [7], we compare the peak acceleration, penetration depth, and collision duration as a function of the initial impact velocity  $v_c$ . We then discuss the results in terms of the unified force law given by Eq. 1. This model is based on the equation of motion and has been shown to accurately describe most impact behaviors [9, 10, 11].

$$F = mg - f(z) - h(z)v^2 \quad (1)$$

In Eq. 1,  $F$  is the total force on the projectile,  $m$  is the mass of the projectile,  $g$  is gravity,  $z$  is the displacement of the projectile relative to its position at impact,  $f(z)$  is the frictional drag term, and  $h(z)$  contributes to the inertial drag term. If  $f(z)$  is derived from Coulomb friction and hydrostatic pressure, then Eq. 1 can be non-dimensionalized based on 5 dimensionless groups. These groups are comprised of quantities like the size and density of the projectile, the bulk density and internal friction of the granular material, and gravity [12]. In this study, we discuss collision behavior in terms of the dimensionless Froude number  $Fr$  (Eq. 2), where  $R$  is the radius of the projectile.

$$Fr = v/\sqrt{gR} \quad (2)$$

**Results:** Fig. 1 shows the results of the impact experiments under terrestrial gravity ( $g = 9.81 \text{ m.s}^{-2}$ ) and the impact experiments under low-gravity ( $g = 1.15\text{-}1.21 \text{ m.s}^{-2}$ ) for the 1.5 mm glass bead surface material. Fig. 2 shows the results of the impact experiments and simulation under terrestrial gravity and the results of the simulations under low-gravity ( $g = 0.10 \text{ m.s}^{-2}$ ) for the 10 mm glass bead surface material. The solid and dotted lines in Figs. 1 and 2 represent the theoretical fit for the peak acceleration based on Eq. 1. The theoretical model and the full solutions for  $z_{\text{stop}}$  and  $t_{\text{stop}}$  are presented in [7].

Figs. 1 and 2 show that the projectile acts similarly when impacting either the 1.5 mm or the 10 mm beads. Most notably,  $z_{\text{stop}}$  appears to collapse onto a single curve when plotted as a function of  $Fr$  (Figs. 1b and 2b). The collapse is particularly evident in the case of the 10 mm bead surface material, where simulations were conducted for the full range of Froude number at both gravity levels. When normalized by  $\sqrt{R/g}$ ,  $t_{\text{stop}}$  also collapses onto a single line, demonstrating that the collision duration remains more or less constant for all Froude numbers (Figs. 1c and 2c).

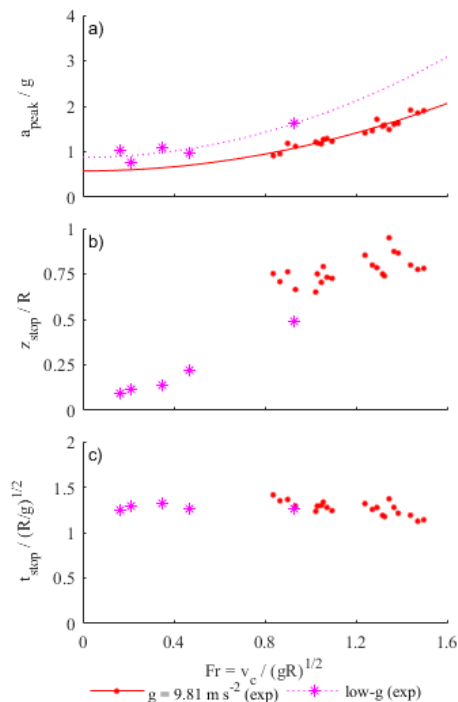


Fig. 1. Evolution of the key collision parameters by Froude number for a spherical projectile impacting 1.5 mm glass beads. The gravity levels in the low-g experiments range from 1.15 to 1.21  $\text{m.s}^{-2}$ . The lines represent the theoretical expression for the peak acceleration based on Eq. 1 and the solution derived in [7].

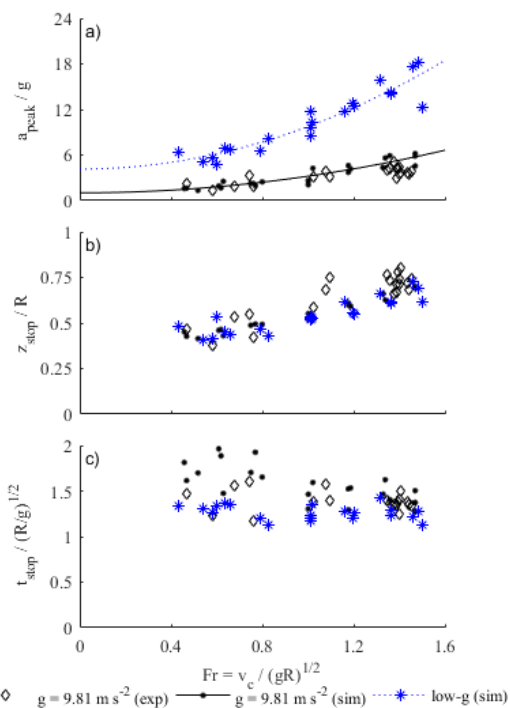


Fig. 2. Evolution of the three key collision parameters by Froude number for a spherical projectile impacting 10 mm glass beads. The low-g simulations were performed for  $g = 0.10 \text{ m.s}^{-2}$ . The lines represent the theoretical expression for the peak acceleration based on Eq. 1 and the solution derived in [7].

**Discussion:** As observed by the solid and dotted lines in Figs. 1a and 2a, the fit for the peak acceleration is different for the terrestrial and reduced-gravity test cases. This means that the derived theoretical solutions for the penetration depth and collision duration will fail to explain the collapse observed in the other plots, as was previously observed in [7]. However, describing collision behavior in terms of the Froude number may help to clarify the relationship between gravity and the collision parameters in order to improve upon the existing theoretical models. Our results, as well as work from previous authors [13], suggest that the method is appropriate.

These results indicate that, for a given material, both the penetration depth and the collision duration can be described in terms of the Froude number. In other words, a 10 cm projectile impacting a granular material with an effective gravity of  $5 \times 10^{-6} \text{ m.s}^{-2}$  (the predicted surface gravity for Dimorphos, the target of the upcoming DART and Hera missions [3, 14]) with a collision velocity of  $0.1 \text{ m.s}^{-1}$ , should experience the same penetration depth and collision duration as a 10 cm projectile impacting the same granular material at  $140 \text{ m.s}^{-1}$  under terrestrial gravity.

Further work is required to understand how the peak accelerations vary with Froude number, and whether the Froude number remains a suitable scaling parameter for larger ranges of effective gravity and different material properties.

**Acknowledgements:** This study has been performed in the framework of the the European Commission H2020 NEO-MAPP project (Near Earth Object Modelling and Payloads for Protection; H2020/SU-SPACE-23-SEC-2019) and uses HPC resources from CALMIP under grant allocation 2020-P20020. CS acknowledges funding from ISAE-SUPAERO and CNES.

**References:** [1] Arakawa et al. (2020) *Science*, 368, 67. [2] <https://www.planetary.org/planetary-radio/1028-2020-dante-lauretta-osiris-rex> [3] Cheng et al. (2018) *PSS*, 157, 104. [4] Michel et al. (2020) *EPSC*, #EPSC2020-103. [5] Campagnola et al. (2018) *Acta Astronautica*, 146, 409 [6] Sunday et al. (2016) *Review of Scientific Instruments*, 87. [7] Murdoch et al. (2021) *Monthly Notices of the Royal Astronomical Society*, submitted. [8] Sunday et al. (2020) *Monthly Notices of the Royal Astronomical Society*, 498. [9] Tsimring and Volfson (2005) *Powders and Grains*. [10] Katsuragi and Durian (2007) *Nature Physics*, 3, 420. [11] Goldman and Umbanhowar (2008) *Physical Review E*, 77. [12] Katsuragi (2016) *Physics of Soft Impact and Cratering*. [13] Wright et al. (2020) *Icarus*, 351, 113963. [14] Michel et al. (2018) *Adv. Space Research*.